Three years of operation of the Chandra X−ray Observatory

Martin C. Weisskopf

Space Science Department, NASA/Marshall Space Flight Center

ABSTRACT

The on−orbit performance of the Chandra X−Ray Observatory over its first three years of observations is reviewed. Operations are running smoothly and the scientific return continues to be exciting and outstanding.

Keywords: **Keywords:** x−ray imaging, grazing−incidence optics, x−ray astronomy.

1. INTRODUCTION

The Chandra X−Ray Observatory is a NASA facility that provides scientific data to the international astronomical community in response to proposals for its use. Data becomes public at most one year after the observation. The Observatory is the product of the efforts of many commercial, academic, and government organizations in the United States and Europe. NASA's Marshall Space Flight Center (MSFC) manages the Project and provides Project Science; TRW Space and Electronics Group served as prime contractor responsible for providing the spacecraft, the telescope, and assembling and testing the observatory; the Smithsonian Astrophysical Observatory (SAO) provides technical support and is responsible for ground operations including the Chandra X−Ray Center (CXC).

2. THE OBSERVATORY

In 1977, NASA/MSFC and SAO began the study leading to the definition of the then named Advanced X−Ray Astrophysics Facility mission. This study, in turn, had been initiated as a result of an unsolicited proposal submitted to NASA in 1976 by Prof. R. Giacconi (Harvard University and SAO) and Dr. H. Tananbaum (SAO). Several significant events took place during the intervening years including the highest recommendation by the National Academy of Sciences Astronomy Survey Committee, selection of the instruments, selection of the prime contractor, demonstration of the ability to build the optics, restructuring of the mission, selecting the name of the mission in honor of the Nobel Prize winner Subramanyan Chandrasekhar, and the launch.

The launch took place on July 23, 1999 by the Space Shuttle Columbia. The Commander was Col. Eileen Collins, the first female commander of a Shuttle flight. With a second rocket system, the Inertial Upper Stage (IUS) attached, the Observatory was both the largest and heaviest payload ever launched by and deployed from a Space Shuttle. Once deployed, and after separating from the IUS, the flight system illustrated in Figure 1 is 13.8−m (43.5−ft) long by 4.2−m (14−ft) diameter, with a 19.5−m (64−ft) solar−panel wingspan. With extensive use of graphite−epoxy structures, the mass is 4,800 kg (10,600 pounds).

The IUS performed two firings and separated from the Observatory. Finally, after five firings of the internal propulsion system − the last of which took place 15 days after launch − the Observatory was placed in its highly elliptical orbit. This orbit has an apogee of 140,000 km (1/3 of the way to the moon) and a perigee of 10,000 km. The inclination to the equator is 28.5°. The satellite is above the radiation belts for more than 75% of the 63.5−hour orbital period.

The spacecraft is standard except for its lightweight construction and provides pointing control, power, command and data management, thermal control, and other such services to the scientific payload. The principal elements of the payload are the x−ray telescope, the scientific instruments, and the aspect system used to determine where the observatory was pointed.

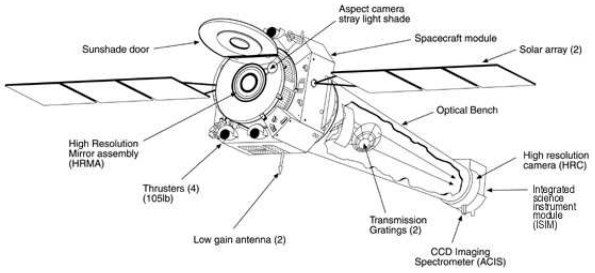

Figure 1. The Chandra X−Ray Observatory.

The specified design life of the mission is 5 years; however, the only perishable (gas for maneuvering) is sized to allow operation for more than 10 years. NASA has recently officially recognized a 10−year mission. The orbit will be stable for decades.

3. USEAGE AND EFFICIENCY

The observing efficiency is dominated by the time spent in the radiation belts at altitudes below about 60,000 km. Other impacts are solar activity, maneuver time, etc. Figure 2 summarizes one year of operations and is typical.

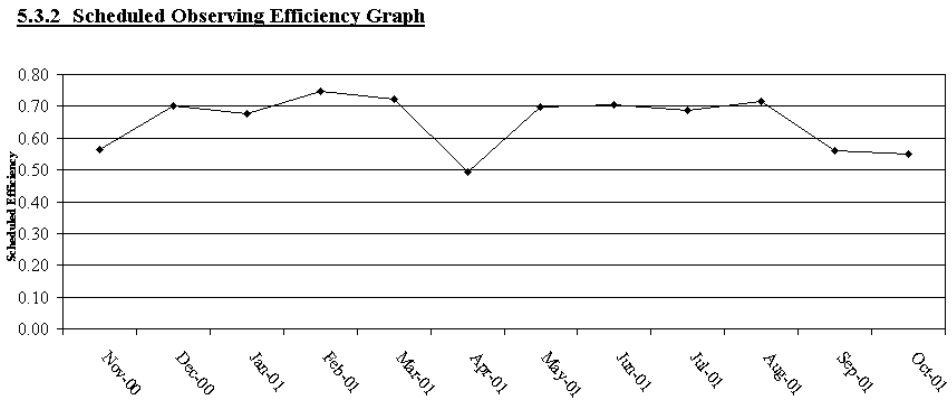

Figure 2. Observing efficiency (time on target) for one year of operation.

NASA has recently completed the review of proposals in response to the fourth announcement. There were 827 Observing Proposals from 20 countries. These included 46 Large Projects (those that require 300 ksec or more), 39 proposals to use the Chandra archives, 28 proposals to perform theoretical research that has direct impact on the analysis and interpretation of Chandra data. The peer review accepted 239 observing proposals of which 11 were large projects. In addition, 20 archive and 9 theory proposals were accepted. Figure 3 illustrates the international participation

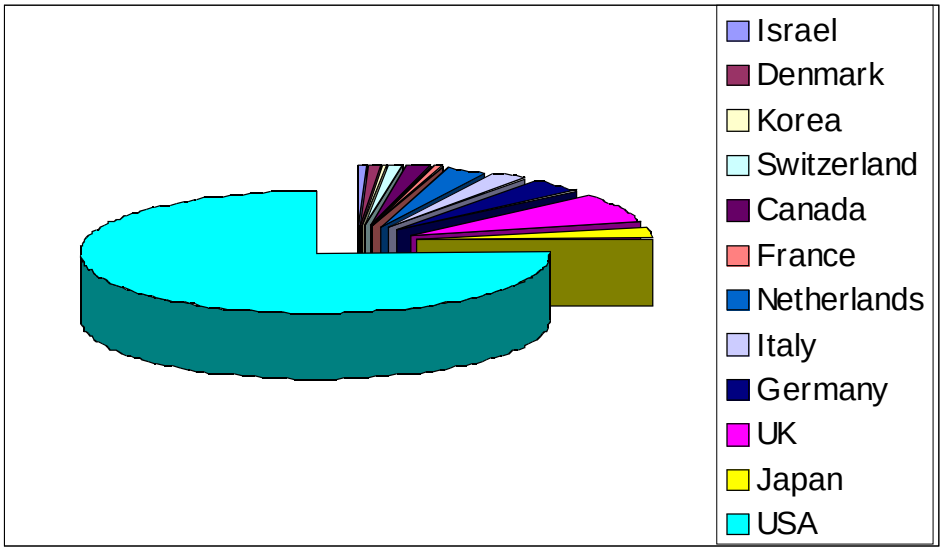

Figure3. Country of origin of the Chandra Principal Investigators for observing cycle 4.

4. INSTRUMENTATION

The first x−rays focused by the telescope were observed on August 12, 1999. Figure 4 shows one of the first images. This image included a new discovery − the bright visible point near the center was the first detection of the compact star (probably a neutron star) created during the implosion of the more massive progenitor. Discoveries of new astronomical features in Chandra images have been the rule, not the exception.

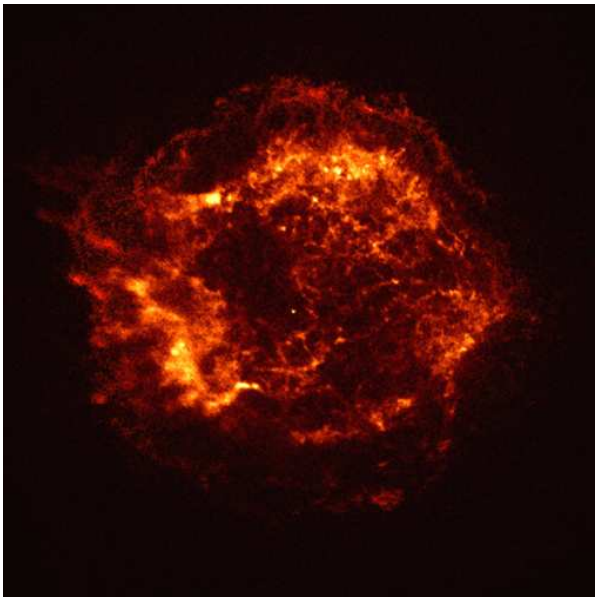

Figure 4. Chandra image of Casseopeia−A. Courtesy NASA/CXC[1].

The Chandra optics and detectors provide, for the first time, sub−arcsecond imaging, sub−arcsecond spectrometric imaging, and, together with transmission gratings, high−resolution x−ray spectroscopy. With these capabilities, a wide variety of high−energy phenomena in a broad range of astronomical objects are being observed. The telescope is made of four concentric, precision−figured, superpolished Wolter−1 x−ray telescopes, similar to those used for both the

Einstein and Rosat observatories, but of much higher quality, larger diameter, and longer focal length. The Wolter−1 design uses a paraboloid of revolution followed by a hyperboloid of revolution. Two reflections minimize coma. The 4−mirror−pair grazing−incidence optic is constructed of Zerodur, a glassy ceramic chosen for its high thermal stability. The mirrors are coated with iridium, chosen for high reflectivity at the x−ray energies of interest, 0.08 − 10.0−keV (15−0.12 nm).

The aspect camera system includes a visible−light telescope and CCD camera attached to the x−ray telescope. A fiducial−light transfer system is used to project lights attached to the focal−plane instruments onto the aspect camera. Thus, the aspect camera simultaneously determines both where the observatory was pointing and the location of the x−ray detector positions relative to the pointing direction. The aspect solution's accuracy depends on the number of stars detected in the field, but is typically 0.6 seconds of arc.

The science instrument module includes mechanisms for focusing and translating the focal−plane instruments. Translation of the instruments is required as x−ray beam−splitters are not very efficient.

Just behind the telescope are 2 objective transmission gratings − the Low−Energy Transmission Grating[2] (LETG), optimized for longer x−ray wavelengths and the High−Energy Transmission Grating[3] (HETG), optimized for shorter wavelengths. Positioning mechanisms may insert either grating into the converging beam to disperse the x−radiation onto the focal plane producing high−resolution spectra read−out by one of the detectors. The gratings allow for measurements with spectral resolving power of $\lambda/\Delta\lambda = E/\Delta E > 500$ for wavelengths of > 0.4−nm (energies < 3 keV).

The Space Research Institute of the Netherlands and the Max−Planck−Institut fur Extraterrestrische Physik designed and fabricated the LETG. The assembly is made of 540 grating facets with gold bars of 991−nm period. The LETG provides high−resolution spectroscopy from 0.08 to 2 keV (15 to 0.6 nm).

The Massachusetts Institute of Technology (MIT) designed and fabricated the High−Energy Transmission Grating (HETG). The HETG uses 2 types of grating facets − the Medium−Energy Gratings (MEG) which, when inserted, are placed behind the telescope's 2 outermost shells, and the High−Energy Gratings (HEG), behind the 2 innermost shells. The HEG and MEG are oriented at slightly different dispersion directions. With polyimide−supported gold bars of 400−nm and 200−nm periods, the HETG provides high−resolution spectroscopy from 0.4 to 4 keV (MEG, 3 to 0.3 nm) and from 0.8 to 8 keV (HEG, 1.5 to 0.15 nm).

Chandra's two focal−plane science instruments are the High Resolution Camera[4] (HRC) and the Advanced CCD Imaging Spectrometer (ACIS)[5].

SAO designed and fabricated the HRC. One of the HRC detectors is made of a 10−cm−square microchannel plate, and provides high−resolution imaging over a 31−arcmin−square field of view. A second detector, comprising 3 rectangular segments (3−cm−by−10−cm each) mounted end−to−end along the grating dispersion direction, serves as the primary read−out detector for the LETG. Both of the HRC detectors are coated with a cesium−iodide photocathode and have thin aluminized polyimide shields to prevent contamination by ions and ultraviolet light.

The Pennsylvania State University MIT built the Advanced CCD Imaging System (ACIS) with charge−coupled devices (CCDs) fabricated by MIT's Lincoln Laboratory. As with the HRC, there are two detector systems. One is made of a 2−by−2 array of CCDs, and provides high−resolution spectrometric imaging over a 17−arcmin−square field of view. The other, a 6−by−1 array mounted along the grating dispersion direction, serves as the primary read−out detector for the HETG. Two types of CCDs were used, 8 front−illuminated (FI) and two back−illuminated (BI). The latter CCDs have higher efficiency at lower energies than the FI devices, but were much more difficult to fabricate. One BI CCD was placed at the on−axis focal position of the 6 x 1 array. Thus this particular CCD also provides high−resolution spectrometric imaging extending to lower energies, but over a smaller (8−arcmin−square) field than the 2 x 2 array. Both ACIS detector systems have thin aluminized polyimide filters to minimize contamination by visible light.

Despite successful science operations, the Observatory has had to deal with a number of technical difficulties that have had their impact on scientific performance. The front− (not the back−) illuminated ACIS CCDs suffered damage,

which increased the charge transfer inefficiency as a result of bombardment by low energy (100 keV) protons crudely focused by the telescope by means of Rutherford scattering as the Observatory entered the radiation belts. Following a procedure of removing ACIS from the focal plane during radiation belt passages has dramatically minimized subsequent increases in the charge transfer inefficiency. O'Dell et al. discuss the Chandra approach to radiation management in detail elsewhere in these proceedings.

Both ACIS filters, which are close to the coldest (120 °C) surfaces on the observatory, appear to be collecting hydrocarbon contamination at the rate of about one−half an optical depth at the Carbon k−edge per year. Figure 5 illustrates one method of quantifying the impact based on our current understanding of the chemical composition and rate of deposition of the contaminants. Normally, we would plan to bake off the contamination after completing detailed measurements using the Chandra gratings of its composition and rate of accumulation. Use of baking is, however, complicated, by the potential impact on the charge transfer efficiency of the CCDs. Ground experiments will be conducted in September of 2002 before deciding the bake−out strategy.

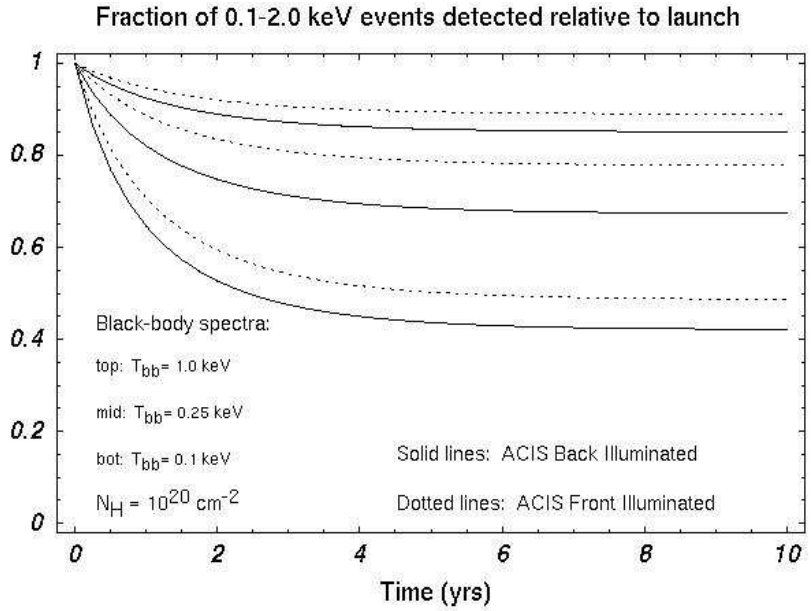

Figure 5. Fraction of detected flux (0.1 to 2.0 keV) for the ACIS BI and FI CCDs for different assumed spectra and the current model of the filter contamination.

5. POINT SPREAD FUNCTION

The Observatory's point spread function, as measured during ground calibration, had a full width at half−maximum less than 0.5 arcsec and a half−power diameter less than 1 arcsec. The pre−launch prediction for the on−orbit encircled−energy fraction was that a 1−arcsec−diameter circle would enclose at least half the flux from a point source. The relatively mild dependence on energy, resulting from diffractive scattering by surface microroughness, attested to the 3 angstroms rms surface roughness The ground measurements were, of course, taken under environmental conditions quite different than those encountered on−orbit. The effects of gravity on the optics and the finite distance and the size of the various x−ray sources used were obviously unique to the ground calibration. On−orbit the performance includes the spatial resolution of the flight detectors and any uncertainties in the aspect solution. The on−orbit performance met expectations as illustrated in Figure 6.

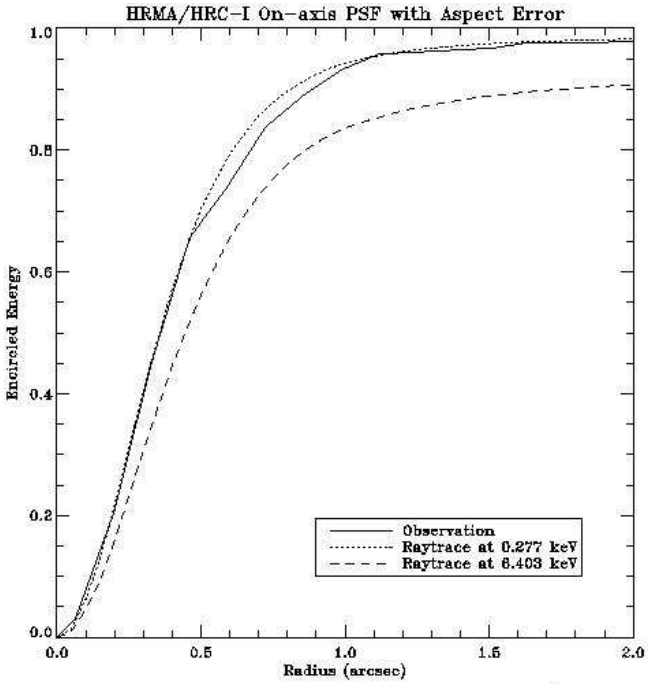

Figure 6. Encircled energy versus radius comparing pre−launch predictions at two energies to on−orbit performance.

The tremendous advancement in angular resolution that the Chandra optics provides, introduces new considerations for the analysis of the data. An example is that now one has to account for the energy dependence of the flux scattered out of the beam by the interstellar medium. Frits Paerels of Columbia University first brought this interesting twist to our attention. The energy dependence of the scattering is contrasted to that of the absorption in Figure 7.

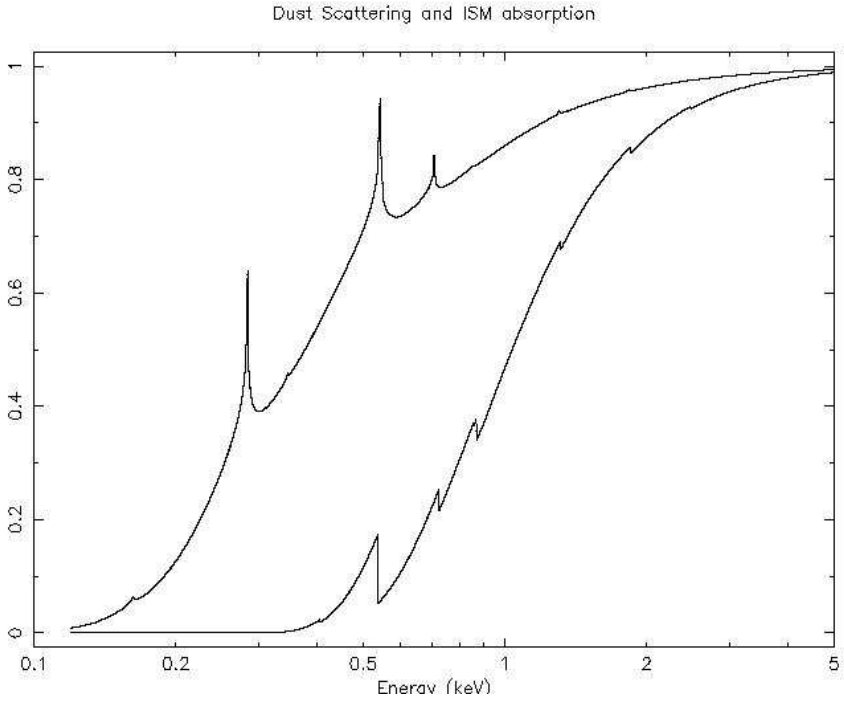

Figure 7. The energy dependence of scattering and absorption by the interstellar medium.

The Observatory's capability for high−resolution imaging enables detailed high−resolution studies of the structure of extended x−ray sources, including supernova remnants, astrophysical jets, and hot gas in galaxies and clusters of galaxies. The additional capability for spectrometric imaging allows studies of structure, not only in x−ray intensity, but also in temperature and in chemical composition. Through these observations, users are addressing several of the most exciting topics in contemporary astrophysics.

In addition to mapping the structure of extended sources, the high angular resolution permits studies of ensembles of discrete sources, which would otherwise be impossible. An example is shown in Figure 8, the Chandra observation of the center of Andromeda (M31). The image shows what used to be considered as the emission associated with the black hole at the center of the galaxy now resolved into several objects. Using also the Hubble Space Telescope (HST), astronomers have now been able to determine the x−ray source associated with the black hole at the center of the galaxy.

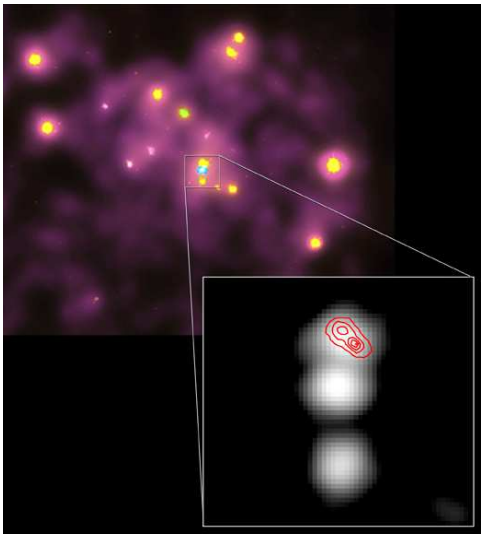

Figure 8. Chandra image of the center of Andromeda (M31). The central region is resolved into 5 distinct sources. The blowup shows the three most central and optical contours from HST observations. X−ray image courtesy NASA/SAO/CXC/M.Garcia et al. The optical contours are courtesy NASA/GSFC/T. Brown et al.

Equally important are Chandra's unique contributions to high−resolution dispersive spectroscopy. As the capability for visible−light spectroscopy initiated the field of astrophysics about a century ago, high−resolution x−ray spectroscopy will contributes profoundly to the understanding of the physical processes in cosmic x−ray sources and is the essential tool for diagnosing conditions in hot plasmas. The high spectral resolution of Chandra isolates individual lines from the myriad of spectral lines, which would overlap at lower.

6. DISCOVERIES

From planetary systems to deep surveys of the faintest and most distant objects, the scientific results from the first three years of Chandra operations have been exciting and outstanding. We conclude this overview with a series of images illustrating some these results. We begin with images of the x−ray emission from the planet Jupiter. Figure 9 shows hot spots at high (and unexpected) latitudes that appear to pulsate at approximately a 45−minute period.[6] In this case the x−rays appear to be produced by particles bombarding the Jovian atmosphere after precipitating along magnetic field lines. Figure 10 continues the discoveries about the Jovian system and shows the first detection of x−rays from two of the moons.[7] Figure 11 shows the fluorescent x−rays arising from Venus's atmosphere being bombarded by solar x−rays.[8]

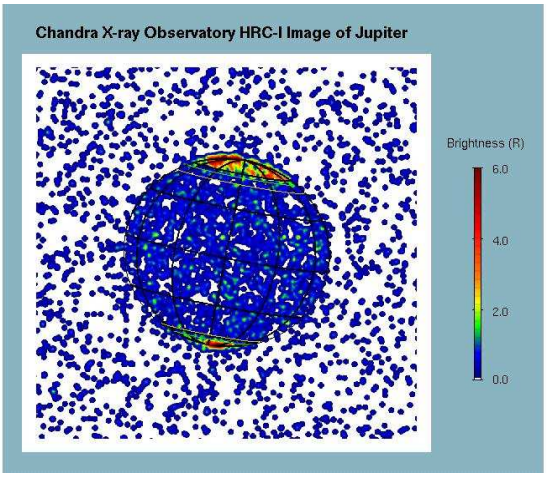

Figure 9. Chandra image of the x−ray emission from Jupiter. Courtesy of R. Elsner.

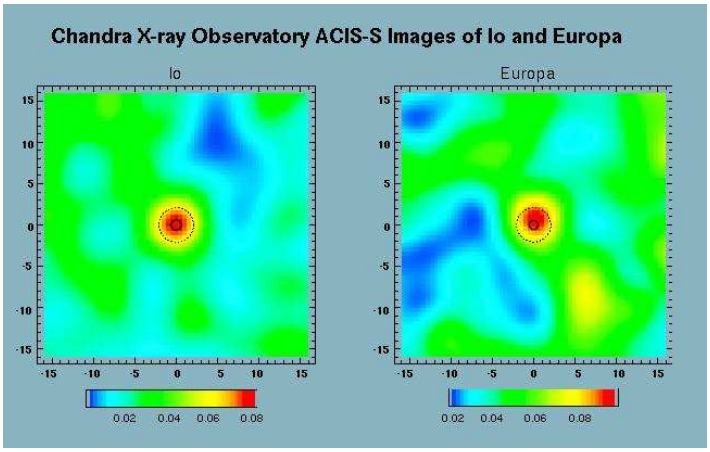

Figure 10. Chandra HRC image of x−rays from the Jovian moons Io and Europa. Courtesy of R. Elsner.

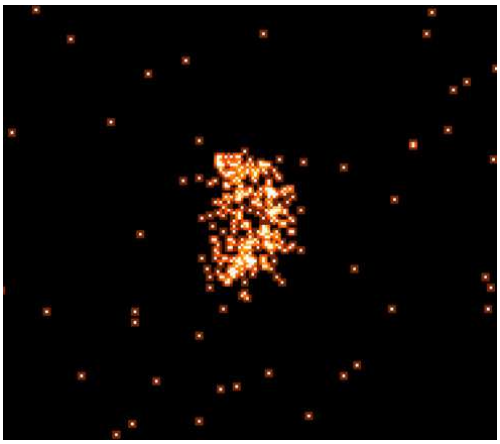

Figure 11. Chandra image of x−rays from Venus. Courtesy of NASA/MPE/K. Dennerl et al.

One of the most spectacular Chandra images is the composite of the center of our own galaxy[9] taken using over 30 overlapping ACIS fields shown in Figure 12. Here we clearly see the presence of both point−like discrete sources (over 1000 of them) and diffuse extended emission. The large amounts of hot gas has been heated and chemically enriched by numerous stellar explosions.

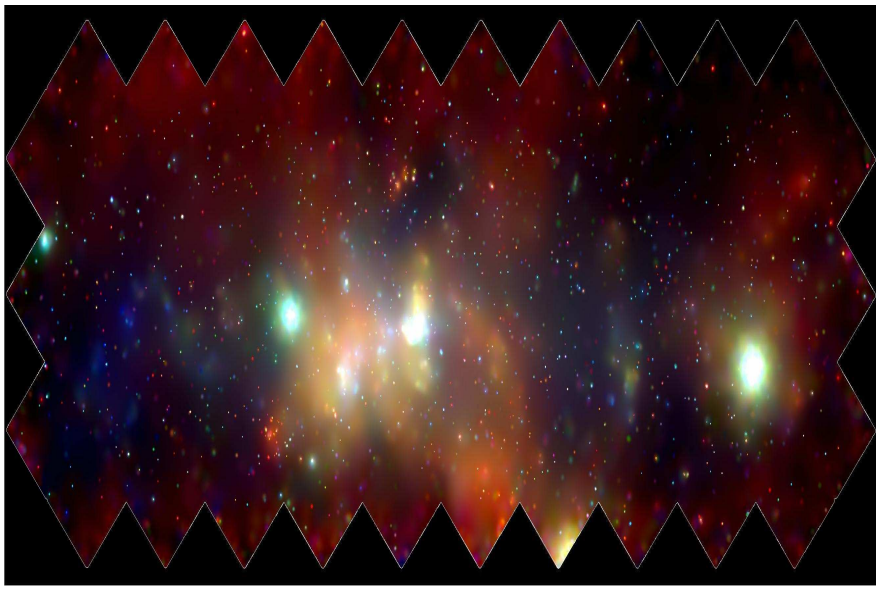

Figure 12. Chandra composite image of the center of the Milky Way galaxy. The image is 120 by 48 arcmin. Courtesy NASA/UMass/Wang et al.

Figures 13 and 14 further illustrate the utility of the superb angular resolution. Figure 13 shows a time history and relative positioning of the optical emission of SNR 1987 A as seen with HST together with the x−ray emission observed with Chandra.[10] The full size of the image is only about 1.5 seconds of arc. Figure 14 shows the Chandra image that resolves two sources in the globular cluster M15[11] that are only 2.7 arcseconds apart.

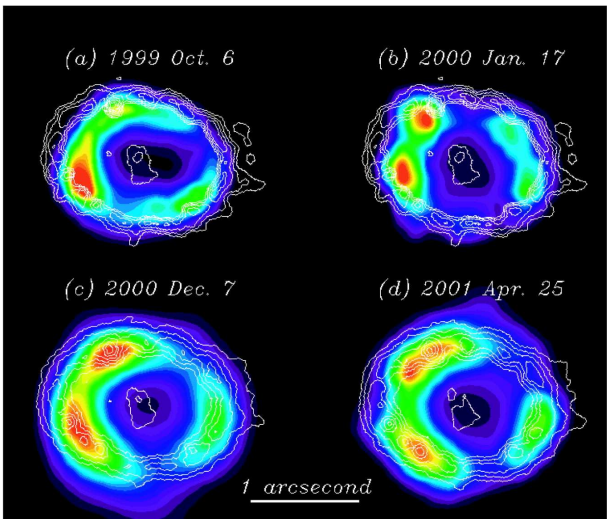

Figure 13. ACIS images and HST contours of the emission from SNR1987A. Courtesy Dave Burrows.

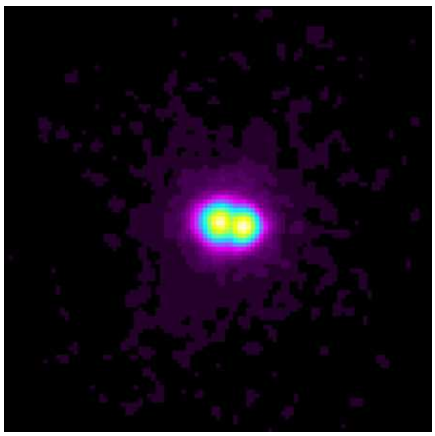

Figure 14. Two x−ray sources in the globular cluster M15. The separation is 2.7 seconds of arc. Courtesy NASA/GSFC/N.White and L.Angelini

The final legacy of Chandra may ultimately be led by the spectroscopic data. The energy resolution, enabled by the quality of the optics, is providing new and extremely complex results. In Figure 15 we show both the zero order and the dispersed images of the supernova remnant E102 obtained with one of the HETG gratings.[12] [13] Dr. Flanagan discusses these data in more detail elsewhere in these proceedings.[3]

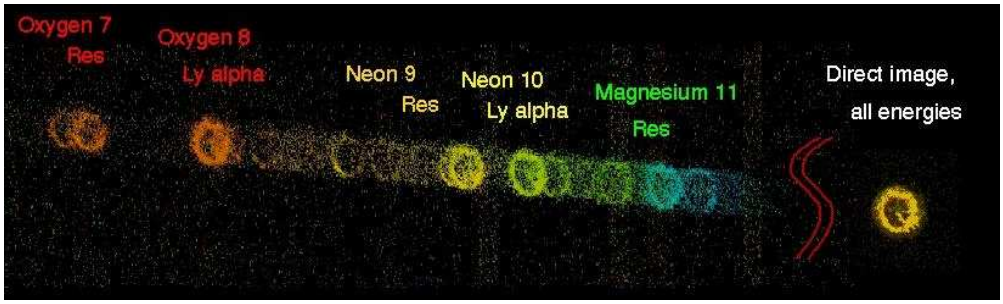

Figure 15.The zero order and a portion of the HETG−dispersed spectrum of the supernova remnant 1E 0102−72. Courtesy Dan Dewey.

In Figure 16 we show the spectacular ACIS image of the Crab Nebula and its pulsar,[14] which revealed, for the first time, the details of the inner structure including the shock front where the pulsar wind is converted to x−rays.

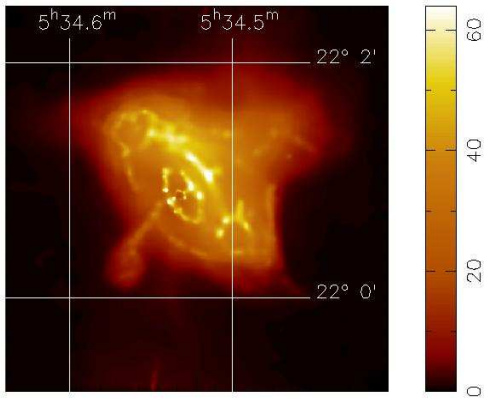

Figure 16. Adaptively smoothed ACIS image of the Crab Nebula and its pulsar.

One of the more important triumphs of the Observatory has been to use the angular resolution and high sensitivity to perform detailed surveys of extended objects such as globular clusters, galaxies, and clusters of galaxies. Figure 17 shows one of the spectacular Chandra images of globular clusters.[15] A survey of a galaxy is illustrated in Figure 18.

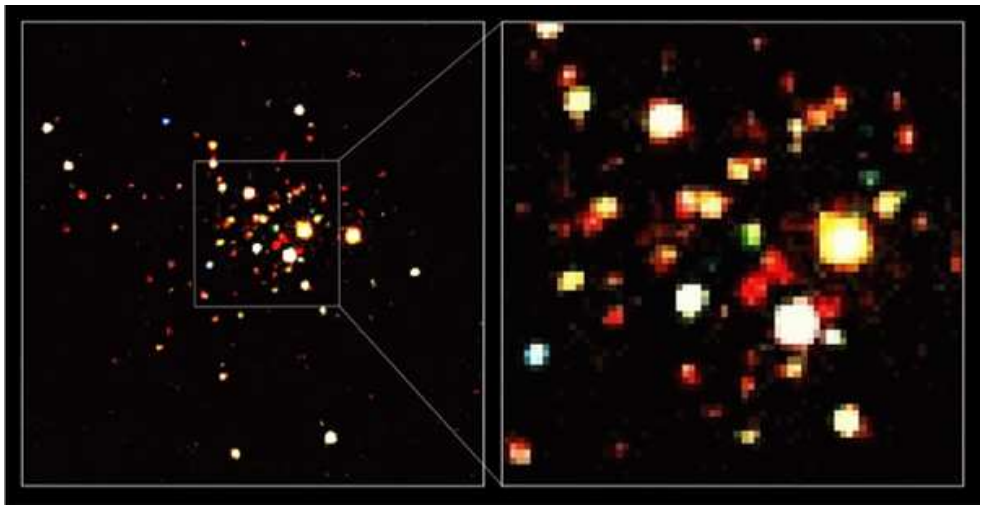

Figure 17. Chandra ACIS image of the globular cluster 47 Tucanae. The left panel covers the central 2’ x 2.5’. The central 35" x 35" are shown to the right. Courtesy NASA/CfA/J.Grindlay et al.

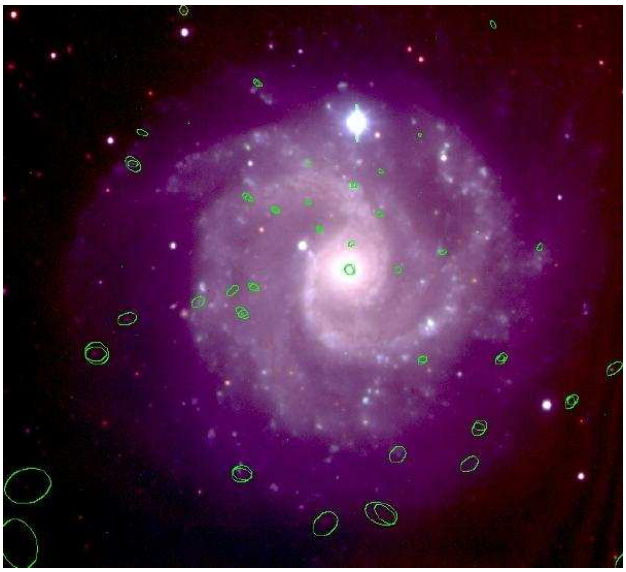

Figure 18. Chandra−detected x−ray sources overlaid on an optical image of NGC 3184. Courtesy Andrea Prestwich.

Chandra observations of clusters of galaxies frequently exhibit previously undetected structures with characteristic angular scales of a few arc seconds. Figure 19 of the Perseus cluster[16] is a spectacular example.

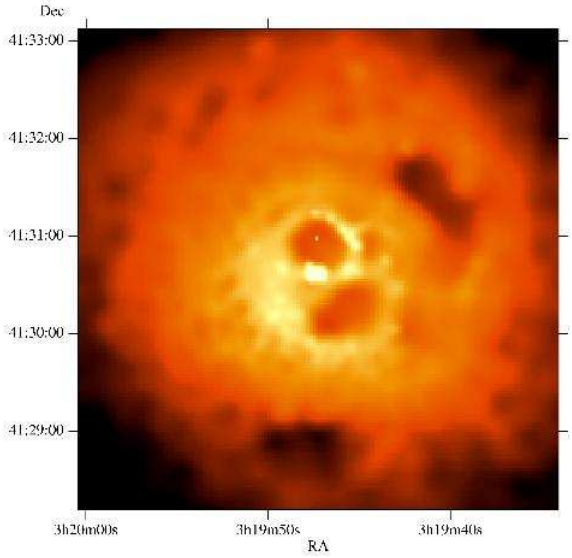

Figure 19. X−ray core of the Perseus cluster. Courtesy NASA/IoA/A. Fabian et al.

Figure 20 illustrates multiwavelength observations of the jets from active galaxies. The Chandra x−ray image[17] shows an irregular, knotty structure similar to that seen at radio and optical[18] wavelengths. However, the knots near the central core are much brighter in X−rays

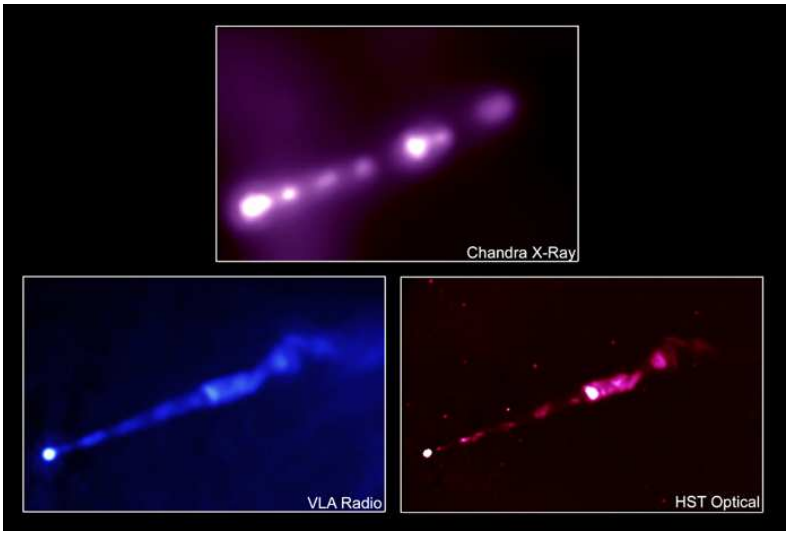

Figure 20. The x−ray jet emanating from the nucleus of the elliptical galaxy M87 as seen in three wavelength bands. Credits: X−ray: NASA/CXC/MIT/H. Marshall et al. Radio: F. Zhou, F.Owen (NRAO), J.Biretta (STScI) Optical: NASA/STScI/UMBC/E.Perlman et al.

High−resolution spectra of Seyfert galaxies are providing new details about the physical and dynamical properties of material surrounding the active nucleus. In the case of Seyfert 1s, whose signal is dominated by a bright X−ray continuum from the central engine, the partially ionized circum−source material introduces prominent patterns of absorption lines and edges. Figure 21, e.g. shows a LETG/HRC spectrum of NGC 5548. This spectrum has dozens of absorption lines.[19]

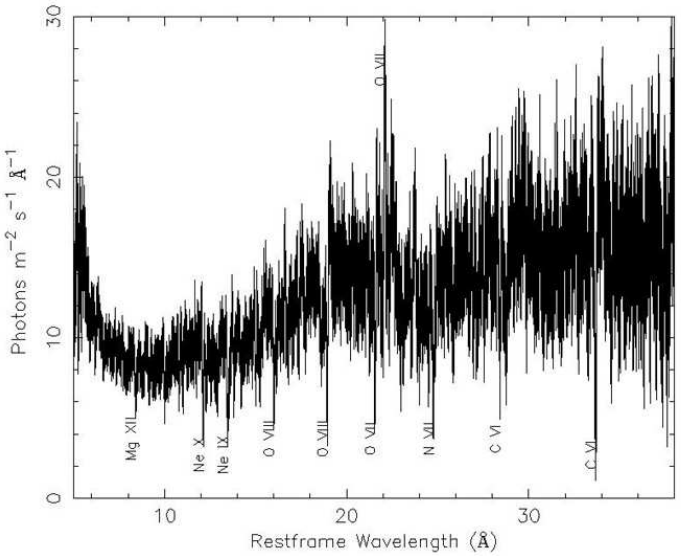

Figure 21. LETG/HRC spectrum[19] of the Seyfert 1 galaxy NGC 5548, corrected for order contamination, redshift and Galactic absorption. Several prominent absorption lines from H−like and He−like ions are marked, as is the forbidden line of He−like oxygen.

For Seyfert 2's the strong continuum from the central engine is not seen directly, so the surrounding regions are seen in emission. Figure 22 provides an example of an LETG/HRC observation of NGC 1068.

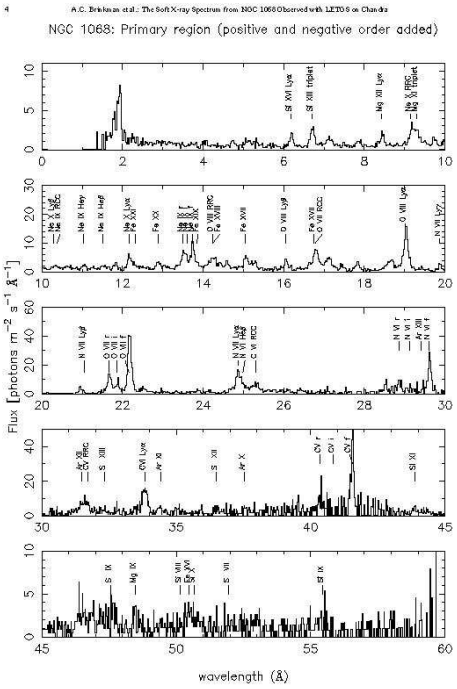

Figure 22. Emission−line spectrum from the Seyfert 2 galaxy NGC 1068.[20] Kindly provided by A. Kinkhabwala .

The Observatory is also being used to search for direct evidence for a warm−hot intergalactic medium (WHIM). Figure 23 illustrates one of these efforts.[21]

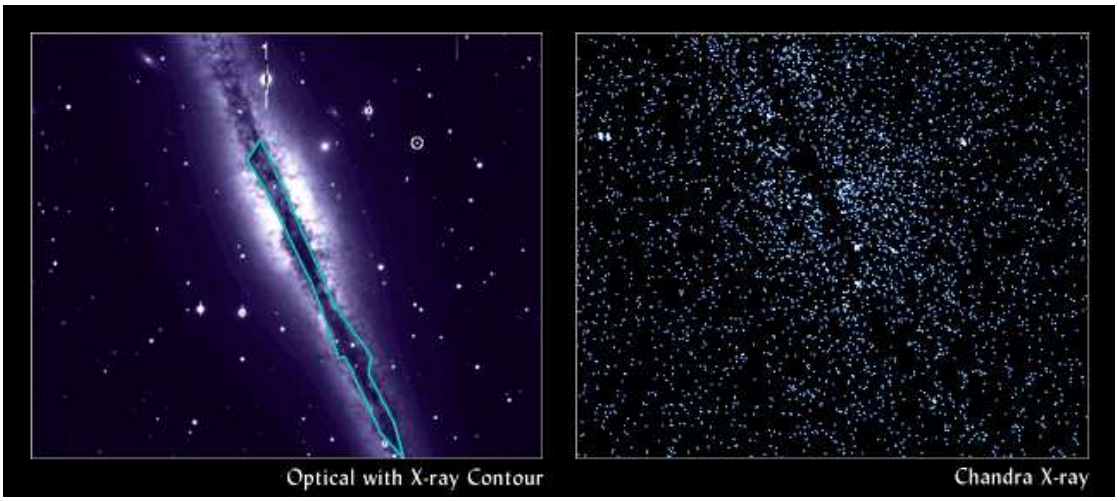

Figure 23. The optical image (left) of NGC 891 shows a dark disk of dust and gas, with a contour outlining the region where the X−ray shadow of the galaxy is darkest. The Chandra image (right) of a shadow cast by the galaxy on an otherwise brighter background of X−rays. The shadow is evidence for a source of X−rays beyond the galaxy and is speculated to arise from the WHIM. Courtesy NASA/CXC/U.Mich./Bregman and Irwin.

No discussion of data taken with the Observatory is complete without a mention of the deep Chandra Surveys. These are deep exposures of particular regions of the sky to study the populations of the objects detected, especially the faintest ones. This work is an outgrowth of the study the diffuse x−ray background, the nature of which had been a puzzle for nearly 40 years, although the lack of distortion of the spectrum of the Cosmic Microwave Background placed a strong upper limit to the possibility of a truly diffuse component[22] Observations with ROSAT at energies below 2 keV made a major step in resolving a significant fraction (70−80%) into discrete objects.[23] Currently two long exposures have been accomplished with the Chandra X−Ray Observatory − the Chandra Deep Fields North[5] with 2 Ms of exposure, and the Chandra deep field south[24] with 1 Msec and depicted in Figure 24. These surveys have extended the study of the background to flux levels more than an order of magnitude fainter than previously in the 0.5−2.0 keV band and have resolved over 90% of the background into a variety of discrete sources. The largest uncertainty in establishing the fraction is now in the knowledge of the total level of the background itself.

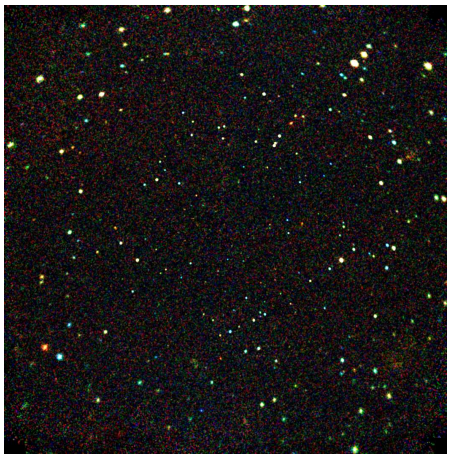

Figure 24. One−million−second image of the Chandra Deep Field South. Courtesy NASA/JHU/AUI/R.Giacconi et al.

7. WORLD−WIDE WEB SITES

The following lists several Chandra−related sites on the World−Wide Web

http://chandra.harvard.edu/: Chandra X−Ray Center (CXC), operated for NASA by the Smithsonian Astrophysical Observatory.

http://wwwastro.msfc.nasa.gov/xray/axafps.html: Chandra Project Science, at the NASA Marshall Space Flight Center.

http://hea−www.harvard.edu/HRC/: Chandra High−Resolution Camera (HRC) team, at the Smithsonian Astrophysical Observatory (SAO).

http://www.astro.psu.edu/xray/axaf/axaf.html: Advanced CCD Imaging Spectrometer (ACIS) team at the Pennsylvania State University (PSU).

http://acis.mit.edu/: Advanced CCD Imaging Spectrometer (ACIS) team at the Massachusetts Institute of Technology.

http://www.sron.nl/missions/Chandra: Chandra Low−Energy Transmission Grating (LETG) team at the Space Research Institute of the Netherlands.

http://www.ROSAT.mpe−garching.mpg.de/axaf/: Chandra Low−Energy Transmission Grating (LETG) team at the Max−Planck Institut fur extraterrestrische Physik (MPE).

http://space.mit.edu/HETG/: Chandra High−Energy Transmission Grating (HETG) team, at the Massachusetts Institute of Technology.

http://hea−www.harvard.edu/MST/: Chandra Mission Support Team (MST), at the Smithsonian Astrophysical Observatory.

http://ipa.harvard.edu/: Chandra Operations Control Center, operated for NASA by the Smithsonian Astrophysical Observatory.

http://ifkki.kernphysik.uni−kiel.de/soho: EPHIN particle detector.

REFERENCES

[1] Pictures that are publicly available at the Chandra web site at http://chandra.harvard.edu have credits labeled "Courtesy of". The acronyms may be found at this site.
[2] See Mendez, M. SPIE, 4851−05 in these proceedings and references therein.
[3] See Flanagan, K. SPIE 4851−04 in these proceedings and references therein.
[4] See Murray, S. S. SPIE 4851−02 in these proceedings and references therein.
[5] See Garmire, G. P. et al. SPIE 4851−03 in these proceedings and references therein.
[6] Gladstone, R. et al. 2002, Nature, Volume 415, pp. 1000−1003.
[7] Elsner, R. F. et al. 2002, The Astrophysical Journal, Volume 572, pp 1077−1082.
[8] Dennerl, K. et al. 2002, Astronomy and Astrophysics, Volume.386, pp 319−330.
[9] Wang, Q. D., Gotthelf, E. V., Lang, C. C. 2002 Nature, Volume 415, pp. 148−150.
[10] Burrows, D. et al. 2000, The Astrophysical Journal, Volume 543, L149. See also SPIE 4851−03 in these proceedings.
[11] White, N. E. and Angelini, L. 2001, The Astrophysical Journal, Volume 561, pp. L101−L105.
[12] Canizares, C. R., Flanagan, K. A., Davis, D. S., Dewey, D., Houck, J. C., and Schattenburg, M. L. 2001, in "Young Supernova Remnants", ed. S. S. Holt and U. Huang, 213.
[13] Flanagan, K. A., Canizares, C. R., Davis, D. S., Dewey, D., Houck, J. C., and Schattenburg, M. L. 2001, in "Young Supernova Remnants", ed. S. S. Holt and U. Huang, 226
[14] Weisskopf, M. C. et al. 2000, The Astrophysical Journal, Volume 536, L81.
[15] Grindlay, J. E., Heinke, C., Edmonds, P. D., and Murray, S. S. 2001, Science, Volume 290, p. 2292.
[16] Fabian, A. C., Sanders, J. S., Ettori, S., Taylor, G. B., Allen, S. W., Crawford, C. S., Iwasawa, K., Johnstone, R. M., and Ogle, P. M. 2000, MNRAS, Volume 318, L65
[17] Marshall, H. L.; Miller, B. P.; Davis, D. S.; Perlman, E. S.; Wise, M.; Canizares, C. R., and Harris, D.E. 2002; The Astrophysical Journal, Volume 564, pp. 683−687.
[18] Perlman, E. S. et al. 2001, The Astrophysical Journal, Volume 561, Issue 1, pp. L51−L54.
[19] Kaastra, J. S., Mewe, R., Liedahl, D. A., Komossa, S., and Brinkman, A. C. 2000, Astronomy and Astrophysics, Volume 354, L83.
[20] Brinkman, A. C., Kaastra, J. S., van der Meer, R. L. J., Kinkhabwala, A., Behar, E., Paerels, F., Kahn, S. M. and Sako, M. 2002, "The Soft X−Ray Spectrum of NGC 1068 Observed with LETGS on Chandra", Astronomy and Astrophysics, submitted.
[21] Bregman, J. N. and Irwin, J. A. 2002, The Astrophysical Journal, Volume 565, Issue 1, pp. L13−L16.
[22] Mather, J. C. et al. 1990, The Astrophysical Journal, Volume 354, L4.
[23] Hasinger, G. et al. 1998, Astronomy and Astrophysics, Volume 329, 482.
[24] Giacconi, R., Rosati, P., Tozzi, P., Nonino, M., Hasinger, G., Norman, C., Bergeron, J., Borgani, S., Gilli, R., Gilmozzi, R., Zheng, W. 2001, Astrophysical Journal, Volume 551, 642.